Research Journal of Chemical Sciences _____ E-ISSN 2231-606X
Vol. **6(4),** 1-11, April **(2016)** *Res. J. Chem. Sci.*

Study of Electron Transfer Path on Reaction of Xanthine Oxidase with 6-Mercaptopurine and Hypoxanthine

Tafesse Bashaye Tessema
Department of Chemistry, Arba Minch University, Arba Minch, Ethiopia
bashayetessema@gamil.com

Available online at: www.isca.in, www.isca.me
Received 28th August 2015, revised 7th December 2015, accepted 8th March 2016

Abstract

Enzymes often rely on the coupling of electrons and protons to affect primary metabolic steps involving charge transport and catalysis. The present theoretical study is intend to explore the path of electron transfer from substrate to active site and to provide a plausible route of electron transfer in the enzymatic catalysis from 6-MP or hypoxanthine to active site. Density functional theory (DFT)/B3LYP method were used to probe the path of electron or proton transfer mechanism from Mullikan charge. The Mullikan atomic charge of Mo decreased from 0.624793 to 0.398834, C_{RH} bound equatorial oxygen of active site is increased by 0.16132, H_{RH} decreased by 0.146701 that is around two fold increase in electron density this may be due to removal of electron as hydride toward sulfido terminal. Terminal sulfido (S_{Mo}-H_{RH}) decreased to -0.0107, O_{eq} of active site decreased to -0.43539 when it bound to C2 of substrate. The electronegativity of O_{eq} more than oxo group by 0.05154 hence O_{eq} is a better nucleophile. Therefore the catalytically labile site should be the metal-coordinated hydroxide (O_{eq}) rather than the apical oxo group (Mo=O). Sulfido terminal (S_{Mo}) decreased in electronegativity due to delocalization of electron density to active site Mo that facilitates the transfer of electron up on the attack of hydride from hydrogen bond substrate. Electron densities on S_{front} and S_{back} increased in (-0.2233 and -0.20266) respectively which may facilitate the movement of equatorial hydroxide towards C2 of substrates (C_{RH}). Charge distribution on C2 is (0.143402 and 0.139523) and on C8 is (0.140514 and 0.133494) respectively for 6-MP and hypoxanthine. This implies in both cases C2 shows electron deficiency and hence it is more electrophilic relative to C8. Charge density of H_{RH} bound C2 is (0.171649 and 0.15786) and H_{RH} bound C8 is (0.08821 and 0.080245) respectively for 6-MP and hypoxanthine hence hydrogen bound C2 is labile for hydride transfer due to high electronegative nature which indicate C2 position is more susceptible to nucleophilic attack by hydroxide of active site. Therefore it can be generalized that oxidation of 6-mercaptopurine or hypoxanthine by XO proceed through abstraction of proton by Glu_{1226} from equatorial hydroxide of active site followed by nucleophilic attach on C2 of substrate and hydride was transferred through concomitant release of oxidized substrate.

Keywords: Hypoxanthine, 6-Mercaptopurine, Density functional theory, Nucleophile.

Introduction

Molybdenum Enzymes: Enzymes that possess molybdenum in their active sites catalyze biological processes that are essential to the organism; indeed neither plants nor animals can survive without molybdenum[1]. The Molybdenum cofactor (Moco) as shown below: consists of mononuclear molybdenum coordinated by the dithiolene moiety of a family of tricyclic pyranopterin structures, the simplest of which is commonly referred to as molybdopterin[2,3].

The co-factor modulates the reduction potential of the molybdenum center and facilitates interaction between the molybdenum center and substrate. A significant feature of the molybdenum center is its coordination to the cis dithiolene sulfur atoms that is the only mechanism for anchoring the metal to the protein[4]. Molybdenum containing enzymes are classified into three families of enzymes Figure-2 below based on the structure of their molybdenum active site and the reaction they catalyze. Xanthine oxidoreductase Figure-2a involved in purine catabolism and aldehyde oxidases (AOs) belong to the same family of xanthine oxidase[5].

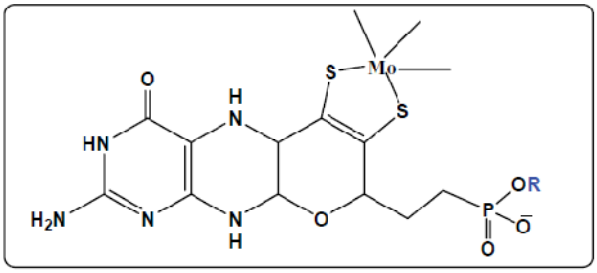

Figure-1
Molybdenum cofactor. R = H for eukaryotic enzymes and R = AMP, CMP or GMP for prokaryotic enzymes. Where AMP: Adenosine monophosphate, CMP: Cytosine monophosphate, GMP: Guanine monophosphate[3]

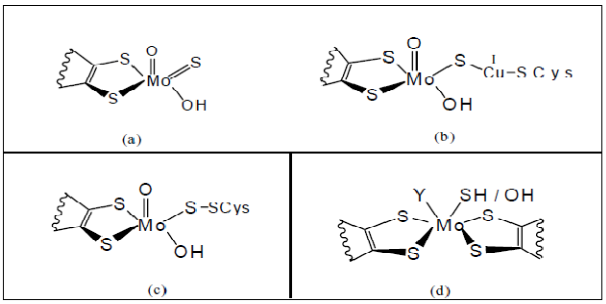

Figure-2
Active site structures of the three families of molybdenum enzyme[6,7]; (a) XO: Xanthine oxidase family, XDH: Xanthine dehydrogenase and (b) CODH: Carbon monoxide dehydrogenase; (c) SO: Sulfite oxidase family (d) DMSOR: Dimethylsulfoxide reductase family. Y represent ligands such as Cys=Cysteine, SeCys= Selenocysteine, Ser = serine, Asp = Aspartic acid

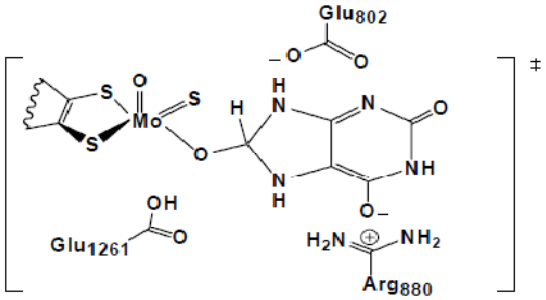

Figure-3
Proposed role of amino acid residues (Glue1261, Arg880 and Glu802) for xanthine bound active site XO in transition state[12]

The Reaction Mechanism of Xanthine Oxidase Enzyme: Mechanism begins with the extraction of a proton from the hydroxyl of the molybdenum center by Glu_{1261}[8] an event computed to occur readily in the presence of the substrate[9]. The electrons from the deprotonated oxygen are then free to attack the electrophilic C8 atom of the bound xanthine as a substrate. The formation of glutamic acid stabilizes this structure through hydrogen bond interactions[10]. The interactions of Arg_{880} and Glu_{802} appear to vary with analogous substrates and inhibitors, leading to the development of two different modes of substrate binding. One mechanism suggests that Glu_{802} forms hydrogen bond interactions with the C6 carbonyl and N7 of xanthine while Arg_{880} forms hydrogen bonds with the carbonyl of C2[11]. The second mechanism suggests an inverted orientation of the substrate allowing for hydrogen bond interactions between Arg_{880} and the C6 carbonyl of xanthine. Crystallographic data suggested possible stabilizing interactions between Arg_{880} of the active site andenolate tautomerisation at C6[12] as shown in Figure-3[12].

The transfer of electrons can be monitored through the formation of the paramagnetic transient Mo(V)[13]. Reaction begins by nucleophilic attack of the Mo-OH(H) on the C8 position of substrate, with either discrete formation of a tetrahedral intermediate followed by hydride transfer to the Mo=S group or hydride transfer concomitant with the initiating nucleophilic attack (via a tetrahedral transition state)[14]. The redox reaction is facilitated by difference in redox potential and electron affinity of the enzyme, substrate and other prosthetic groups, the electron affinity of the enzyme cofactors approximately follows FAD. With a few exceptions, enzymes of the xanthine oxidase family contain a molybdenum cofactor (Moco) and $[Fe_2S_2]$ clusters catalyze the oxidative hydroxylation of a range of aromatic heterocyclic compounds and aldehydes (RCHO) in reactions that involve the cleavage of a C-H bond[15].

Currently accepted mechanism of reductive half reaction of xanthine oxidase with physiological substrate xanthine is postulated to take place through a base-assisted nucleophilic reaction[16] as shown in Scheme-1.

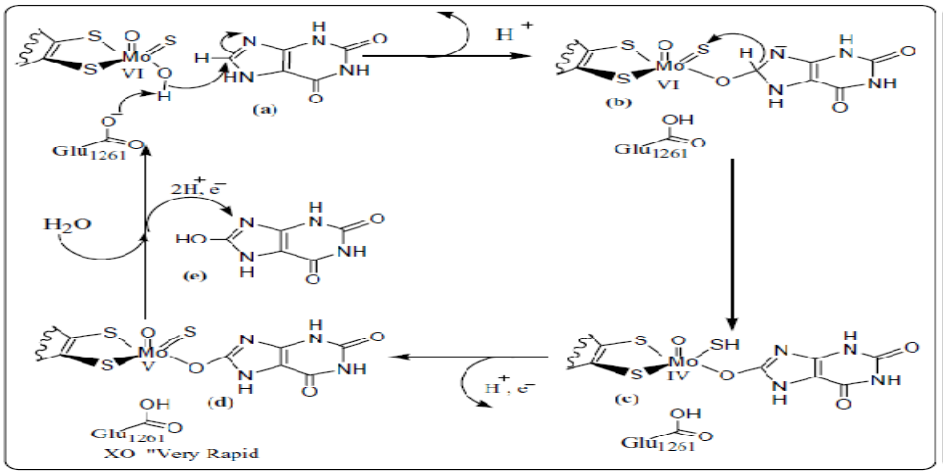

Scheme-1
A postulated base-assisted hydride transfer mechanism for the hydroxylation of xanthine by XO enzyme. In the most favorable pathway, the [bm XOR]-Glu1 261 is proposed to act as a general base[17]

Purine substrates hydroxylated at a specific carbon position in a reaction initiated by nucleophilic attack of an equatorial Mo-OH group. Deprotonation is thought to be facilitated by a conserved glutamate residue ($Glue_{1261}$ in the bovine enzyme), as shown in Scheme-1[8]. Up on nucleophilic attack on substrate carbon (C_{RH}) atom the sp^2 hybridized carbon atom is re-hybridized from sp^2 to sp^3 to give tetrahedral complex. The active site pocket itself is lined by several conserved residues: Glu_{802}, Leu_{873}, Arg_{880}, Phe_{914}, Phe_{1009}, and Glu_{1261}[18]. The several hydrophobic residues, Leu_{873}, Phe_{914}, and Phe_{1009}, serve to form the active site pocket[8].

Oxidation of 6-Mercaptopurine and Hypoxanthine: The oxidation of hypoxanthine is theorized to occur much like the oxidation of xanthine. Hence the mechanism begins with the extraction of a proton from the hydroxyl of the molybdenum center by Glu_{1261}. The deprotonated molybdenum oxygen is then free to undergo a nucleophilic attack on C2 of hypoxanthine paired with the concomitant hydride transfer from hypoxanthine to the molybdenum bound sulfido terminal. The reactive species are stabilized by hydrogen bond interactions between the protonated Glu_{1261}. The study on hypoxanthine shows, it is found in the gas phase as a mixture of two predominant tautomeric forms: the (N1-H, N9-H) and (N1-H, N7-H) keto-species Figure-5. According to the relative stabilities of tautomers, it is suggested that the "bioactive" species corresponds to the (N1-H, N9-H) ketotautomer[19]. The subsequent electron transfer and product release occur similarly to the xanthine oxidation reaction[10].

Therefore if hypoxanthine replaces xanthine it proceeds through similar reaction mechanism. Chemotherapeutic agent 6-MP and the Physiological substrate hypoxanthine Figure-5 below are analogous heterocyclic species. Hypoxanthine is formed by fusing aromatic pyrimidine ring and imidazole to form purine as shown in Scheme-2 above. When 'R' groups of purine derivative, R1= OH and R2=H hypoxanthine is obtained and oxygen on C6 of hypoxanthine is replaced by sulfur 6-MP is formed this implies structurally they have a close similarity as shown in Figure-5.

As mentioned above oxidation of hypoxanthine occur much like the oxidation of xanthine then the structural analogue 6-MP will hydroxylated in similar fashion like hypoxanthine. Xanthine have sp^2 hybridized electrophilic carbon that hydroxylated by xanthine oxidase. Hypoxanthine as well as 6-MP also has sp^2 hybridized electrophilic carbon. Therefore if xanthine is replaced by hypoxanthine or 6-MP they undergo similar reaction with xanthine oxidase but may passes through different intermediate as shown in Scheme-2.

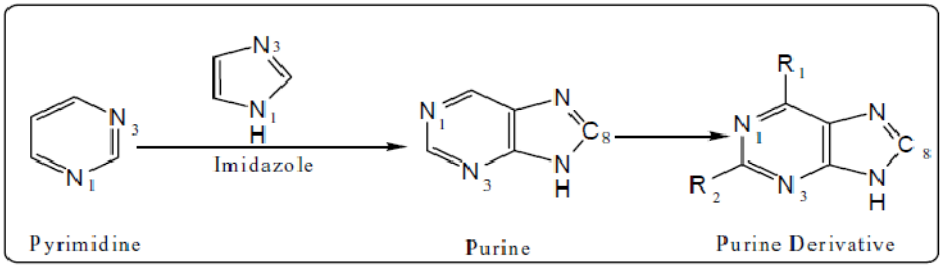

Scheme-2

Heterocyclic reducing substrates purine derivatives. (Purine derivative includes: purine if R1 and R2=H, Hypoxanthine if R1=OH and R2= H, 6-methylepurine if R1=CH3 and R2=H, 2-hyroxyy-6-methylpurine if R1=CH_3 and R2=OH and Xanthine if R1=OH and R2=OH

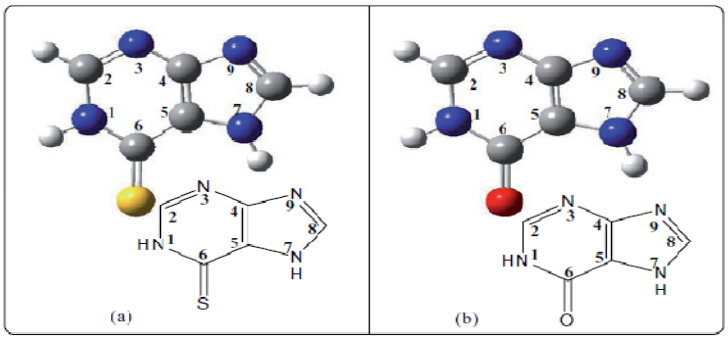

Figure-4

Structural analogous of purine (a) 6-mercaptopurine (b) Hypoxanthine (ChemDraw)[13], they are model substrates for this study

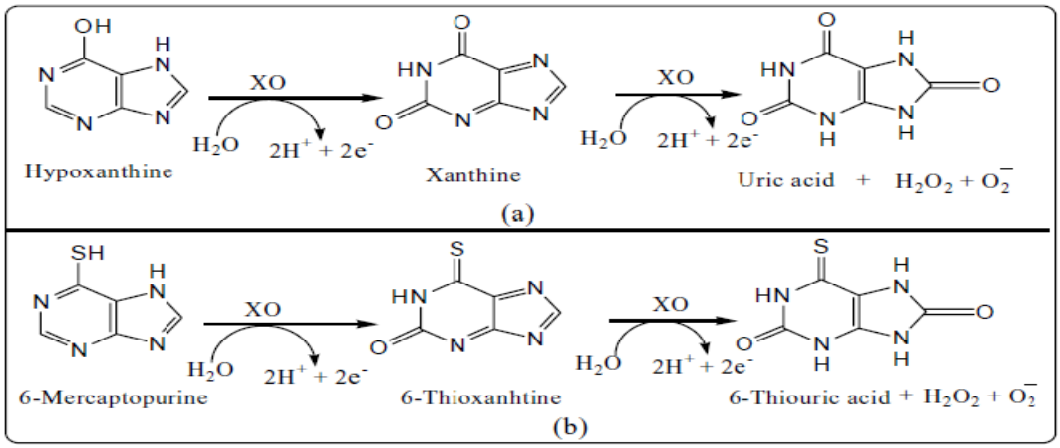

Scheme-3

(a) Oxidative hydroxylation of hypoxanthine to xanthine and xanthine to uric acid, (b) Oxidative hydroxylation of 6-mercapto purine to 6-thioxanthine to 6-thiouric acid[20]

Physiological substrate hypoxanthine and the chemotherapeutic agent 6-MP have two alternate orientations in the active sites. Due to the presence of two C2 and C8, Figure-4 above sp^2 hybridized electrophilic carbons. Crystal structure shows that both the overall orientations of substrate and positions of the several active site amino acids are very similar for hypoxanthine and 6-mercaptopurine, except that Thr_{1010} appears to hydrogen bond to N1 or N7 (for the orientations with C2 and C8 proximal, respectively) of hypoxanthine but not to 6-MP. This appears due to a rotation of 6-MP by approximately 15° to accommodate the larger sulfur atom at the C6 position[12]. The binding stage from the currently accepted general mechanism proceeds through nucleophilic attack by active site on C8 of xanthine to form tetrahedral complex as shown in Scheme-4. The binding stage for 6-mercaptopurine or hypoxanthine can be represented similarly as Scheme-4 above.

Therefore from Scheme-1 and 4 it can be concluded that tetrahedral complex could be formed in the binding stage of all xanthine, hypoxanthine and 6-MP. The tetrahedral complex is stable intermediate in purine hydroxylation step; hence the reaction transformed to transition state as it does in case of xanthine bound active site XO.

The transfer of the proton and electron can occur in either a stepwise or concerted pathway[21]. In the stepwise mechanism, either the proton or electron may be transferred first[22]. Hydrogen atom transfer (HAT) commonly recognized as a radical pathway, in which electron and a proton originating from the same atom[23]. Proton-coupled electron transfer (PCET) is especially prevalent at metallo-cofactors that activate substrates at carbon, oxygen, nitrogen and sulfur atoms.

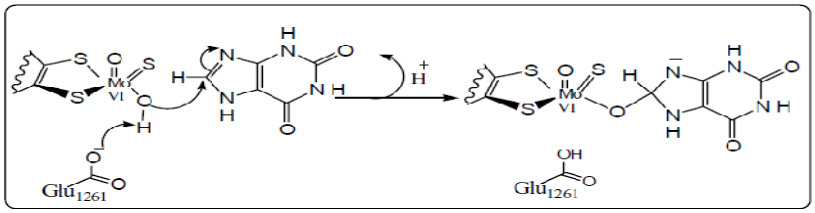

Scheme-4

Currently accepted reaction mechanism for binding stage of xanthine bound active site xanthine oxidase

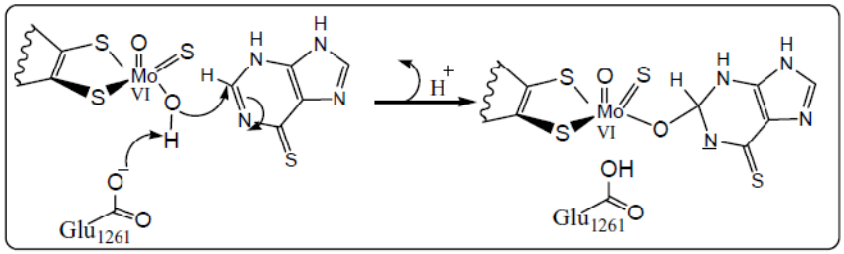

Scheme-5

Proposed reaction mechanism for binding stage of 6-mercaptopurine or hypoxanthine bound active site xanthine Oxidase

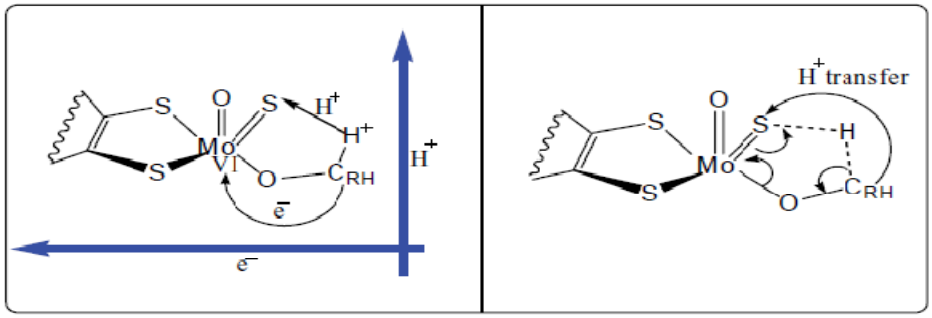

Scheme-6

Orthogonal PCET, C_{RH} represents the substrate (6-mercaptopurine) vertical arrow show the direction of proton transfer and horizontal arrow shows the transfer of electron

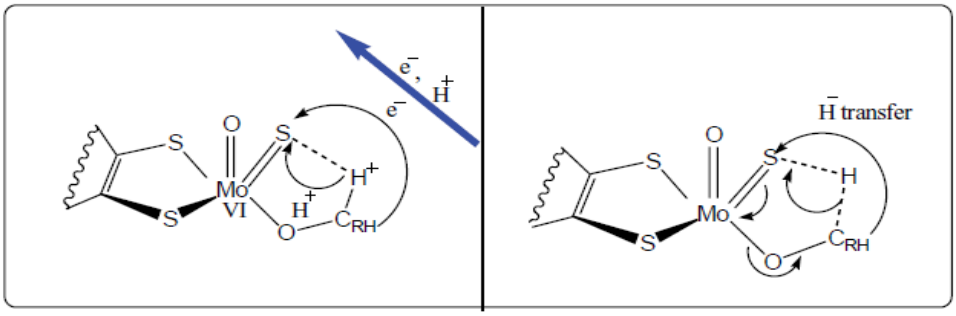

Scheme-7

Collinear PCET, C_{RH} (6-mercaptopurine), arrow show the direction of electron and proton transferred[25]

The PCET reactions depend on the redox potential, E, and the pKa. The redox potential determines the rate of electron transfer, while the pKa influences the rate of the proton transfer[24].

The above proton, electron and hydrogen atom transfer can be generalized into three categories. I. hydride transfer: collinear transfer of two electrons and a proton from substrate C2 to sulfido terminal S_{Mo} Scheme-7. II. Hydrogen atom transfer (HAT): when a proton and an electron transferred collinear from substrate to sulfido terminal and the remaining one electron is passed through equatorial oxygen to metal center and III. Proton transfer: when proton is transferred through sulfido terminal and two electrons through equatorial oxygen which is called orthogonal PCET Scheme-6[16].

Materials and Methods

Materials: Structures were developed using GaussView 3.0 and CS Chem3D pro 1999 (Cambridge Soft Corp., Cambridge, MA, U.S.A.). All Calculations were performed using Gaussian 03W (version 6.0) program software package (Gaussian, Inc., Wallingford, CT, U.S.A.).

The inputs were prepared for submission to Gaussian and to examine graphically the output of (Optimized molecular structures, molecular orbital, atomic charges, and animation of normal model corresponding to vibrational frequencies) and other Gaussian products were visualized using software programs such as GaussView 3.0 (Gaussian, Inc., Pittsburgh, PA, U.S.A.).

Methods: Density functional theory (DFT) was applied to optimize the structures. Becke's three- parameter exchange function and the Lee, Yang and Parr correlation functional (B3LYP) method were employed in the DFT calculations. The 6-31G (d', p') basis set with a polarization function was used for non-metal atoms (C, H, O, N, and S). Similarly, LANL2DZ (Los Alamos National Laboratory 2 Double Zeta) effective core potential (ECP) basis sets were used for Mo atoms.

Predicting the transition state structures: The general structure shown in Figure-5 was used to predict the transition state structures.

The substrate (C_{RH}) in Figure-5 was replaced by 6-MP or hypoxanthine as shown below in Figures-6 with up and down conformations. The transition state was determined by linear transit calculation through linear motion of hydrogen bound substrate (H_{RH}) during the migration of hydrogen (H_{RH}) from substrate (C_{RH}) C2 to sulfide terminal (Mo=S) of xanthine oxidase.

The transition state structures were characterized by: transition state energies, Frequency calculation, Mullikan charge and bond length analysis.

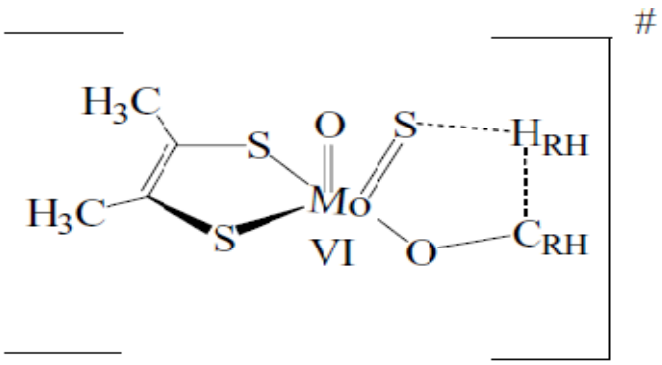

Figure-5
A general structure for the transition state

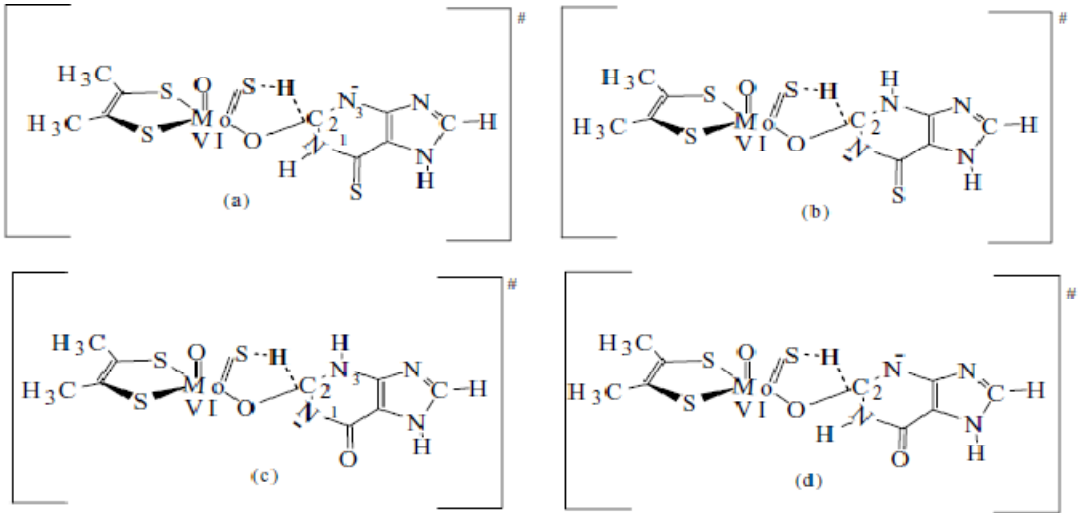

Figure-6
The geometries represent the transition state structures of MoVI state of truncated Moco bound: (a) 6-mercaptopurine up, (b) 6-mercaptopurine down (c) hypoxanthine down and (d) hypoxanthine up

The geometries were modeled in (a) N-up (b) N-down, (c) N-down, and (d) N-up conformations. N-up and down, represents the negative charge on N3 is above and on N1 is below the equatorial plane of 6-mercaptopurine or hypoxanthine bound truncated molybdenum cofactor (Moco).

The bond distance the input files used for linear transit calculation of the substrates (6-mercaptopurine or Hypoxanthine). Run 1: the initial substrate bound active site xanthine oxidase to be optimized (2.27427Å), Run 2 the second substrate bound active site xanthine oxidase to be optimized (S_{Mo}-H_{RH} =2.14223Å), Run 8: the eighth substrate bound active site xanthine oxidase to be optimized (SMo-H_{RH} = 1.35Å). The Mullikan atomic charges for series of eight optimized structures including transition state structure were evaluated for all complexes interns of transition state energy, frequency, Mullikan charge, and bond length analysis.

The electrophilic carbons of the substrates were compared from Mullikan atomic charge and orbital hybridization. For this purpose the two substrates 6-MP and hypoxanthine were optimized. The structures of the input structure were given in Figure-7.

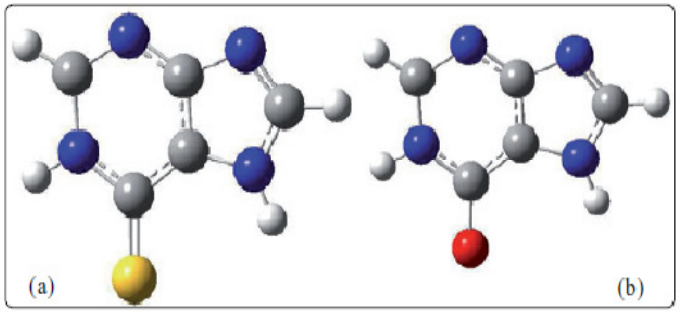

Figure-7
(a)The input structures of 6-MP and (b) hypoxanthine for the generation of charge distribution for electrophilic carbon and the bond distance o f the reactants to compare with substrate bound active site

Path of Electron Transfer: The path through which electron

transferred from substrate to active site studied by careful analysis of the change in Mullikan atomic charge as H_{RH} migrates from C2 of 6-MP or hypoxanthine to the active site of sulfido terminal.

Results and Discussion

The output from linear transit calculation used to determine the trends of Mullikan atomic charges for selected group of atoms. It is used to characterize the redox reactions and the paths of electron transfer from the substrate to reductive half reaction active site. Mullikan atomic charges of optimized structure were collected from output files of linear transit calculation and charge versus H_{RH}-S_{Mo} distance plots were given in the result section Figure-8 and 9.

The linear transit Mullikan charge profile for selected groups of atoms. The traces designated from top to bottom of right side. Mo (first trace), C_{HR} (second trace), H_{RH} (third trace), and S_{back} dithiolene trans to equatorial oxygen (fourth trace), S_{front} dithiolene trans to sulfido terminal (fifth trace), S_{Mo} terminal sulfido (sixth trace), O_{eq} equatorial oxygen (seventh trace) and Ooxo (eighth trace). The Mullikan atomic charges were calculated during the linear motion of H_{RH} from C_{RH} (C-H) through transition state (TS) to the terminal sulfido S_{Mo}(S-H).

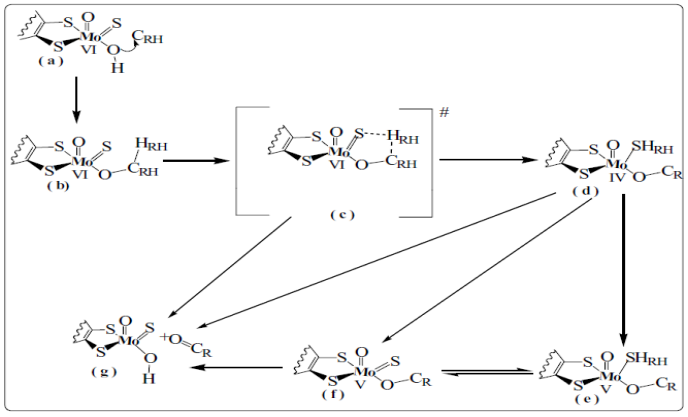

Scheme-8

A hypothetical general schematic model for the catalytic transformation of the oxidation of substrates (C_{RH}) by XO enzymes proceeds through either concerted or stepwise reaction mechanism

The linear transit Mullikan charge profile for selected groups of atoms. The traces designated from top to bottom of right side. Mo (first trace), C_{HR} (second trace), H_{RH} (third trace), and S_{back} dithiolene trans to equatorial oxygen (fourth trace), S_{front} dithiolene trans to sulfido terminal (fifth trace), S_{Mo} terminal sulfido (sixth trace), O_{eq} equatorial oxygen (seventh trace) and Ooxo (eighth trace).

The Mullikan atomic charge of Mo of substrate bound active site is (0.624793), in the transition state it is (0.391551) decreased by (0.233242), still it is electropositive with value ranging from 0.624793 to 0.398834 as compared to other coordinated atom showing its metallic character which showed no change after transition state as indicted in Figure-8 first trace. The change in Mullikan charge of Mo indicates the accumulation of charge in its reduced state Mo(IV) in the reductive half reaction which is oxidized to Mo(VI) up on oxidative half reaction. Equatorial oxygen (O_{eq}) of active site at the beginning is (-0.55619), in transition state its charge is (-0.44026), decrease the electron density by (0.11593) and again decreased to (-0.43539) when it bound to C2 of substrate. The charge density for equatorial oxygen decreased or become less electronegative as it moves from active site to substrate hence the possibility of electron transfer from substrate to active site through equatorial oxygen, orthogonal proton coupled electron transfer Scheme-6 may be ruled out. Apical oxo (Mo=O) showed no significant change in Mullikan atomic charge relative to other atoms as it form a straight trace for the migration of H_{RH}. The Mullikan atomic population of Oxo group (Mo=O) is (-0.50465), that of equatorial oxygen (O_{eq}) is (-0.55619), O_{eq} negative than oxo group by (0.05154). Even if the difference is not so large it can be concluded that Oeq is a better nucleophile for its higher negative charge. Therefore the catalytically labile site should be the metal-coordinated hydroxide (O_{eq}) rather than the apical oxo group (Mo=O). This is consistence with theoretical study[26] and in addition to its less electronegativity the X-ray structure analysis showed that lack of enough space for the substrate to approach the Mo center from the axial direction[26] which is other factor that may decrease its reactivity.

The Mullikan atomic charge of terminal sulfido (S_{Mo}) is (-0.46586) for substrate bound active site, in the transition state it is (-0.34216) decreased or become less electronegative by (0.1237) and finally when S_{Mo} bound hydrogen (H_{RH}) of substrate it is increased to (-0.36711). The decrease in electronegativity may suggest delocalization of electron density to active site Mo that facilitates the transfer of electron up on the attack of hydride from hydrogen bound substrate. The same trend is observed for both mercaptopurine and hypoxanthine as shown in Figure-8 and 9.

The charge of dithiolene sulfurs, sulfur back (S_{back}) for substrate bound active site is (-0.14252), at transition state decreased to (-0.1899) by (0.04731) and finally decreased or become more electronegative to (-0.20266) as H_{RH} bound S_{Mo}. The charge of sulfur front (S_{front}) at the beginning is (-0.14187), at transition state decreased to (-0.21479) by (0.07292) and finally decreased or become more electronegative to (-0.2233) as H_{RH} bound S_{Mo}. The decrease in charge is larger for sulfur front (S_{front}) by (0.08143) as H_{RH} migrates from C_{RH} to S_{Mo} than S_{back} which is decreased by (0.06014) and S_{front} greater than S_{back} by (0.02064); this is probably back bonding of metal in plane d_{xy} orbital with sulfur out of plane p_z orbitals which may delocalize electron between S_{back} and Mo. The electron density of S_{back} may favored towards Mo in order to induce oxygen transfer and modulate electron density on oxidized and reduced forms of active site, this explains the influence of trans effect of S_{back} to facilitate

O_{eq} transfer. The S_{front} experience less synergic effect as it cis to O_{eq}. In general the increase in electronegativity may be attributed by the increase of electron densities on dithiolate sulfur (-0.2233 and -0.20266) S_{front} and S_{back} respectively which facilitate the movement of equatorial hydroxide towards C2 of substrates (C_{RH}). It was indicated by the study of fold angle of dithiolate density at the metal center[27].

The Mullikan atomic charges difference between 6-mp and hypoxanthine. The bar graphs containing C8 and C2 represent 6-mp (left side) and hypoxanthine (right side) from each of the two bars. Substrates are 6-mp (C8: carbon in the eighth position, C2: carbon in the second position as indicated in Figure-4. The same designation was used for Hypoxanthine.

Table-1
Bond Distance for S_{Mo}-H_{RH} (Å)

Run attempted	6-mercaptopurine		Hypoxanthine	
	Up	Down	Up	Down
Run 1	2.274270	2.274270	2.274270	2.274270
Run 2	2.142230	2.142230	2.142230	2.142230
Run 3	2.010190	2.010190	2.010190	2.010190
Run 4	1.851040	1.851040	1.851040	1.851040
Run 5	1.746116	1.746116	1.746116	1.746116
Run 6	1.614078	1.614078	1.614078	1.614078
Run 7	1.482039	1.482039	1.482039	1.482039
Run 8	1.350000	1.350000	1.350000	1.350000

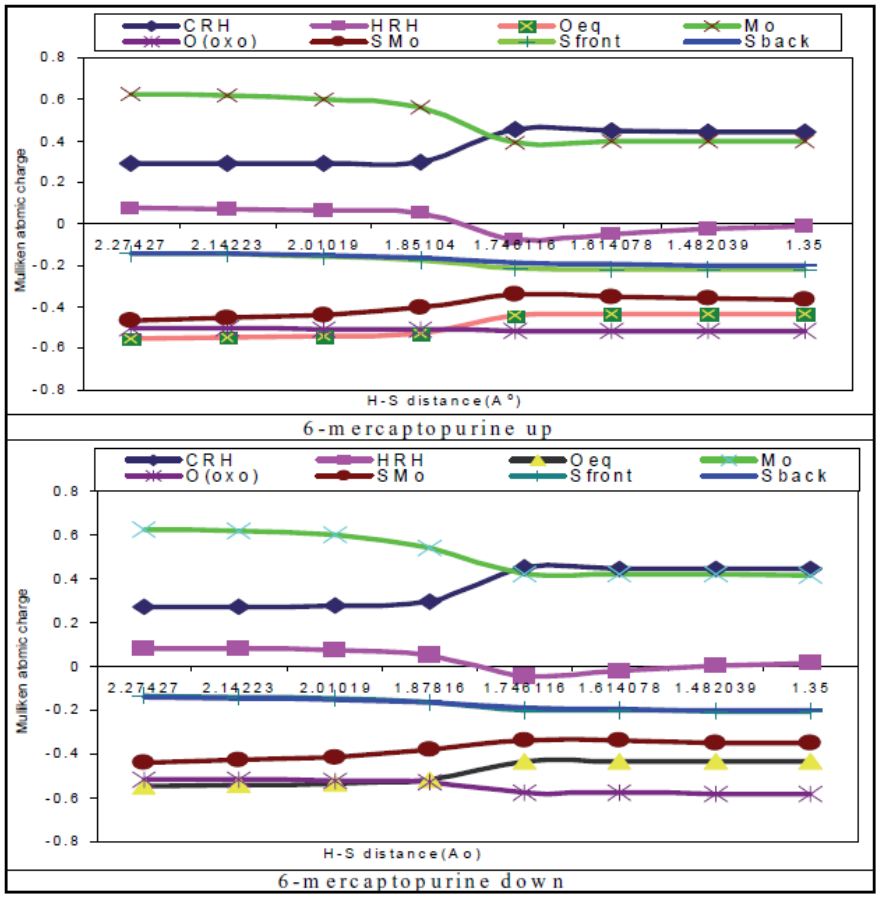

Figure-7
The linear transit Mullikan atomic charges for selected group s of atoms

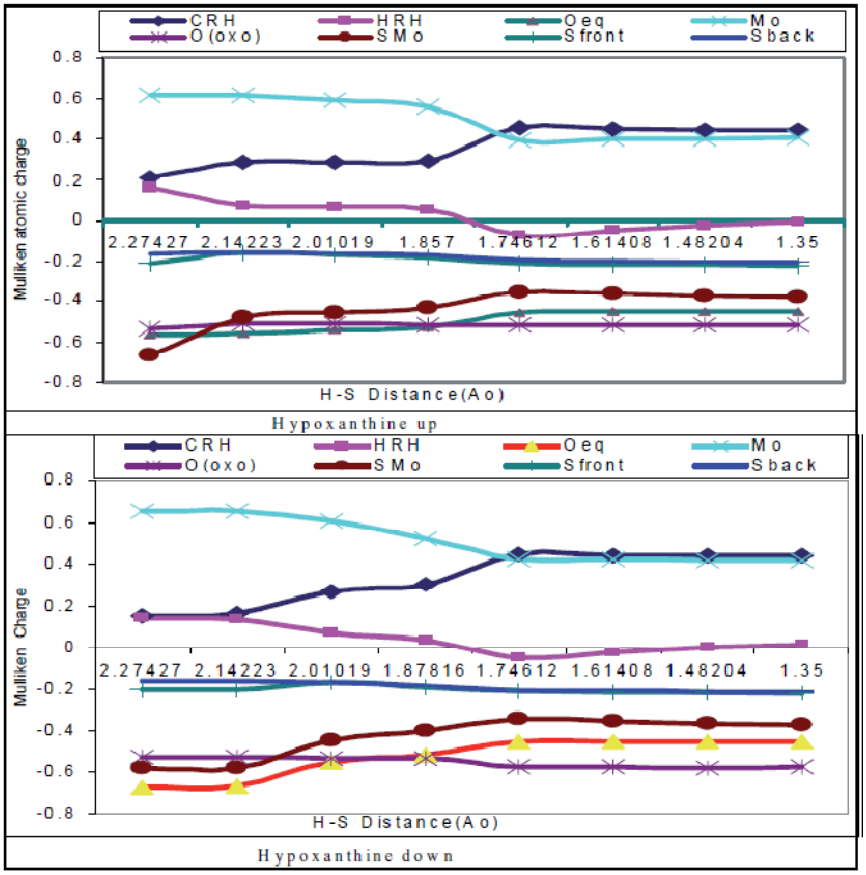

Figure-8
The linear transit Mullikan atomic charges for selected groups of atoms

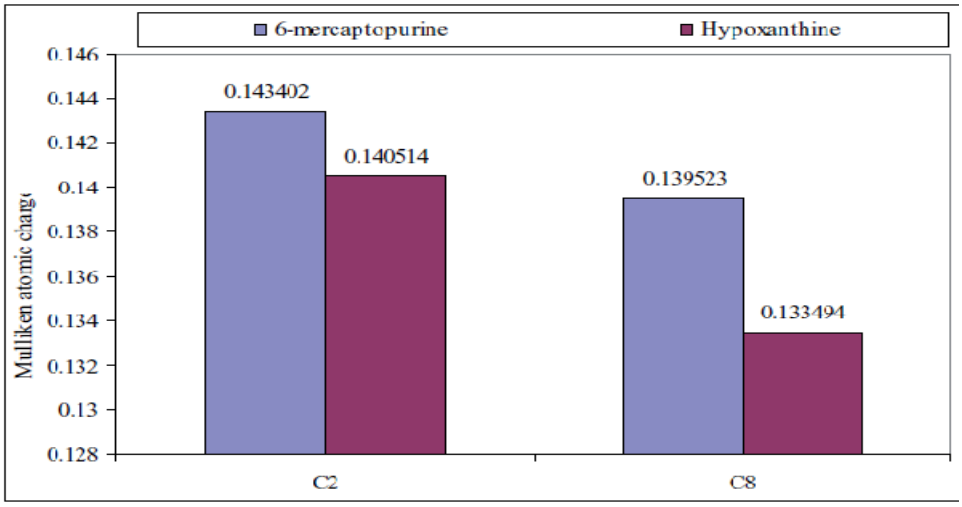

Figure-9
The Mullikan atomic charge distribution for the interaction sites of substrates

The Mullikan population of electrophilic C2 of substrate (C_{RH}) Figure-4 bound equatorial oxygen of active site is (0.29105), in the transition state it is (0.45237) increased by (0.16132). The Mullikan charge for carbon increased or become more positive as O_{eq} approaches and H_{RH} migrates away. This may be due to removal of electron as hydride transferred toward sulfido terminal. The hydride transfer from substrate C2 to sulfido terminal was supported by a number of studies[21]. The Mullikan atomic charge for hydrogen bound C2 of substrate (H_{RH}) is (0.073131) in C_{RH}-H_{RH} and it is (-0.07357) in the

transition state, decreased by (0.146701) that is around two fold increase in electron density. Gradually the negative charge decreased to (-0.0107) as it bound to the terminal sulfido (S_{Mo}-H_{RH}).

Therefore hydroxylation may be initiated by nucleophilic attack of a Mo-OH on the electrophilic C2 Figure-4 of the substrate. There are two possible interaction sites of substrate at the active sit C2 and C8 Figure-4. A DFT calculation of charge distribution for 6-MP is (0.143402 and 0.139523) on C2 and C8 respectively Figure-10. That of hypoxanthine is (0.140514 and 0.133494) on C2 and C8 respectively Figure-10. A MOPAC calculation of charge distribution for the predominant N9-H tautomer of neutral hypoxanthine shows a partial charge of +0.232, on C2 and of -0.002 on C8 was reported[26]. This implies in both cases C2 shows electron deficiency and hence it is more electrophilic relative to C8. Furthermore, the Mullikan atomic charge of hydrogen atoms (H_{RH}) bound C2 of 6-MP and hypoxanthine is (0.171649 and 0.15786) and bound C8 is (0.08821 and 0.080245) respectively. Hydrogen on C2 is labile for hydride transfer due to its electronegative nature for 6-MP or hypoxanthine. Both these factors indicate that the C2 position is more susceptible to nucleophilic attack by hydroxide of active site. Electrophilicity of C2 of 6-MP is greater than hypoxanthine as shown in Figure-10, this implies the interactive site of 6-MP is reactive for nucleophilic attack relative to hypoxanthine. In support of interactive site the study of sequential hydroxylation of hypoxanthine indicated that hypoxanthine is hydroxylated exclusively at the C2 position and C2 of hypoxanthine is comparably reactive as C8 of xanthine[12].

Conclusion

The Mullikan atomic charge of Mo in transition state decreased by (0.233242), which indicate the accumulation of charge in the reductive half reaction that transferred from substrate. Electrophilic C2 of substrate (C_{RH}) increased by (0.16132) this indicates reduction of electron density around C2 indicating hydride is transferred from this species. The Mullikan atomic charge for hydrogen bound C2 of substrate (H_{RH}) is decreased by (0.146701) that is around two fold increase in electron density. On the basis of a substantial negative charge accumulation on the proton in the course of transfer, it can be conclude that the reaction catalyzed by hydride transfer from the sp^2 carbon of substrate to the active site sulfido terminal. The hydride transfer from substrate C2 to sulfido terminal was supported by a number of studies[11]. The charge density on equatorial oxygen (O_{eq}) decreased by (0.11593) and hence the possibility o f electron transfer from substrate to active site through equatorial oxygen, or orthogonal proton coupled electron transfer may be ruled out. The catalytically labile site should be the metal-coordinated hydroxide (Oeq) rather than the apical oxo (Mo=O) for nucleophilic attack. The DFT calculation of this study for charge distribution of interactive carbon shows C2 position is more electrophilic relative to C8. In support of interactive site the study of sequential hydroxylation of hypoxanthine indicated that hypoxanthine is hydroxylated exclusively at the C2 position and C2 of hypoxanthine is comparably reactive as C8 of xanthine[19]. The negative charge accumulated on C6-S- of 6-MP or C6 -O- of hypoxanthine during the transition state stabilized better through the interaction with the positively charged Arg_{880}. It is expected that the abstraction of proton from hydroxide ligand of active site by Glu_{1261} and simultaneous nucleophilic attack of hydroxo group of active site to electrophilic C2 of substrate coexist. The second step is hydride transfer from substrate to sulfido terminal of active site with concomitant release of hydroxo ligand from active site to C2 of substrate takes place.

References

1. Garattini E., Mendel R., Romao M.J., Wright R. and Terao M. (2003). Mammalian molybdo-flavoenzymes, an expanding family of proteins: Structure, genetics, regulation, function and pathophysiology. *Biochem. J*., 372, 15-32.

2. Liu M.T.W., Wuebbens M.M., Rajagopalan K.V. and Schindelin H. (2000). Crystal Structure of the Gephyrin-related Molybdenum Cofactor Biosynthesis Protein MogA from Escherichia coli. *J Bio. Chem*., 3, 1814-1822.

3. Mendel R.R. (2007). Biology of the molybdenum cofactor. *Journal of Experimental Botany*, 58 (9), 2289-2296.

4. Rajagopalan K.V. (1997). The molybdenum cofactors-perspective from crystalstructure. *J Bio. Inorg. Chem*., 2, 786-9

5. Hille R. (2002). Molybdenum and tungsten in biology. *TRENDS in Biochemical Sciences.,* 27(7), 1-8.

6. Huber R., Hof P., Duarte R.O., Moura J.J.G., Moura I., Liu M.Y., LeGall J., Hille R., Archer M. and Romao M.J. (1996). A structure-based catalytic mechanism for the xanthine oxidase family of molybdenum enzymes. *Proc. Natl. Acad. Sci.* USA, 93, 8846-8851.

7. George G.N., Garrett R.M., Prince R.C. and Rajagopalan K.V. (1996). The molybdenum site of sulfite oxidase: A comparison of wild-type and the cysteine 207 to serine mutant using X-ray absorption spectroscopy. *J. Am. Chem. Soc*., 118, 8588-8592.

8. Leimkuhler S., Stockert A.L., Igarashi K., Nishino T. and Hille R. (2004). The role of active site glutamate residues in catalysis of Rhodobacter capsulatus xanthine dehydrogenase. *J. Biol. Chem*., 279, 40437-40444.

9. Amano T., Ochi N., Sato H. and Sakaki S. (2007). Oxidation reaction by xanthine oxidase: Theoretical study of reaction mechanism. *J. Am. Chem. Soc*., 129(26), 8131-8.

10. Okamoto K., Matsumoto K., Hille R.E., ger B.T., Pai E.F. and Nishino T. (2004). The crystal structure of xanthine oxidoreductase during catalysis: Implications for reaction mechanism and enzyme inhibition. *Proc. Natl. Acad. Sci.* USA., 101, 7931-7936.

11. Nishino T., Okamoto K., Eger B.T. and Pai E.F. (2008). Mammalian xanthine oxidoreductase - mechanism of transition from xanthine dehydrogenase to xanthine oxidase. *FEBS J*., 275(13), 3278-89.

12. Kalra S., Jena G. Tikoo and Mukhopadhyay A.K. (2007). Preferential inhibition of xanthine oxidase by 2-amino-6-hydroxy-8-mercaptopurine and 2-amino-6-purinethiol. *BMC Biochemistry*, 8(8), 1-11.

13. Cho I.E.Y., Stockert A.L., Leimkuhler S. and Hille R. (2004). Studies on the mechanism of action of xanthine oxidase. *J. Inorg. Biochem*., 98(5), 841-8.

14. Hille R. (1997). Mechanistic aspects of the mononuclear molybdenum enzymes, *JBIC,* 2, 804-809.

15. Yamaguchi Y., Matsumura T., Ichida K., Okamoto K. and Nishino T. (2007). Human Xanthine Oxidase changes its substrate specificity to Aldehyde Oxidase type upon mutation of amino acid residues in the active site: Roles of active site residues in binding and activation of purine substrate. *J. Biochem*., 141, 513-524.

16. Reece S.Y., Hodgkiss J.M., Stubbe J. and Nocera D.G. (2006). Proton-coupled electron transfer: The mechanistic underpinning for radical transport and catalysis in biology. *Phil. Trans. R. Soc*., B361, 1351-1364.

17. Hernandez B., Luque F.J. and Orozco M. (1996). Tautomerism of xanthine oxidase substrates hypoxanthine and allop urinol. *J. Org. Chem*., 61, 5964-5971.

18. Enroth C., Eger B.T., Okamoto K., Nishino To., Nishino Ta. and Pai E.F. (2000). Crystal structures of bovine milk xanthine dehydrogenase and xanthine oxidase: Structure-based mechanism of conversion. *Proc. Nat. Acad. Sci. USA*., 97, 10723-10728.

19. Kisker C., Schindelin H. and Rees D.C. (1997). Molybdenum cofactor containing enzymes: structure and mechanism. *Annu. Rev. Biochem*., 66, 233-267.

20. Pauff J.M., Cao H. and Hille R. (2009). Substrate Orientation and Catalysis at the Molybdenum Site in Xanthine Oxidase: Crystal structures in complex with xanthine and lumazine. *J. Bio. Chem*., 284 (13), 8760-7.

21. Cao H., Pauff1 J.M. and Hille R. (2010). Substrate orientation and catalytic specificity in the action of xanthine oxidase: The sequential hydroxylation of hypoxanthine to uric acid. *J. Biol. Chem*., Papers in Press page 1-23.

22. Huynh M.H.V. and Meyer T.J. (2007). Proton-Coupled Electron Transfer. *Chem. Rev.,*107, 5004-5064.

23. Mayer J.M. and Rhile I.J. (2004). Thermodynamics and kinetics of proton-coupled electron transfer: Stepwise vs. concerted pathways. *Biochim. Biophys. Acta*., 1655, 51-58.

24. Lingwood M., Hammond J.R., Hrovat D.A., Mayer J.M. and Borden W.T. (2006). MPW1K Performs Much Better than B3LYP in DFT Calculations on Reactions that Proceed by Proton-Coupled Electron Transfer (PCET). *J. Chem Theory Comput.,* 2(3), 740-745.

25. Cukier R.I. (1996). Proton-Coupled Electron Transfer Reactions: Evaluation of Rate Constants. *J. Phys. Chem*., 100, 15428-15443.

26. Joshi H.K., Cooney J.J.A., Inscore F.E., Gruhn N.E., Lichtenberger D.L. and Enemark J.H. (2003). Investigations of metal–dithiolate fold angle effects: Implications for molybdenum and tungsten enzymes. *PNAS*, 100(7), 3719-3724.

27. Yan S., Kang S., Sayashi T., Mukamel S. and Lee Y.J. (2009). Computational studies on electron and proton transfer in phenol-imidazole-base triads. *J. Comput Chem.,* 00, 1-10.